



Environmental application of amine functionalised magnetite nanoparticles grafted graphene oxide chelants

Prateekshya Suman Sahu¹ · Ravi Prakash Verma¹ · Chetna Tewari² · Nanda Gopal Sahoo² · Biswajit Saha^{1,3} 

Received: 7 April 2022 / Accepted: 7 June 2022 / Published online: 16 June 2022
© The Author(s), under exclusive licence to Springer-Verlag GmbH Germany, part of Springer Nature 2022

Abstract

This study proposed a two-step method involving hydrothermal and electrostatic self-assembly processes for synthesising an amine-functionalised magnetic ligand graphene oxide-based nanocomposite (EDTA@Fe₃O₄@GO). The amine groups were successfully attached to the surface of iron (II, III) oxide (Fe₃O₄), which were embedded on the surface of graphene oxide (GO) (Fe₃O₄@GO). This EDTA@Fe₃O₄@GO nanocomposite was used as a chelating agent to bind the toxic heavy metal ions. EDTA@Fe₃O₄@GO demonstrated the synergistic effect between the large surface area and magnetic behaviour of Fe₃O₄@GO and the chelating effect of EDTA, and it showed higher efficiency than the individual GO and Fe₃O₄. The possible structural and compositional characteristics were proposed based on Fourier transform infrared spectra (FTIR), X-ray diffraction (XRD), scanning electron microscope (SEM), Brunauer–Emmett–Teller (BET) and Raman spectroscopy analysis. The outcomes revealed the mechanism behind the excellent As(V) adsorption onto EDTA@Fe₃O₄@GO. The adsorption process was studied by fitting the experimental data obtained into various kinetic and isotherm models. The pseudo-second-order (PSO) kinetic model and the Freundlich isotherm model (FIM) were found to be the best fit models for the removal of As(V) by EDTA@Fe₃O₄@GO. EDTA@Fe₃O₄@GO has the utmost adsorption capacity of 178.4 mg/g. Furthermore, the EDTA@Fe₃O₄@GO nanocomposite is reusable, and it showed excellent adsorption capacity up to 5 cycles. This study has provided insight into the potential of EDTA@Fe₃O₄@GO and its applications in large-scale wastewater treatment.

Keywords Nanocomposite · Graphene oxide · Heavy metal · As(V) · Adsorption

Introduction

Extensive water contamination is among the most severe environmental problem in today's modern world. The widespread release of heavy metals has increased with the advancement of various industries. Toxicity, carcinogenicity, non-biodegradability, and bio-accumulative nature of the

heavy metals have deadly effects on aquatic life and humans (Ezzeddine et al. 2015; Khan et al. 2013). According to World Health Organization (WHO), arsenic (As) is one of the highly toxic heavy metal pollutants that pose maximum adverse effects on human health (Mohammed Abdul et al. 2015). The water bodies and soil are contaminated with this pollutant because of the discharge of untreated water from various industries such as mining, battery, petroleum refining, ceramic manufacturing, agricultural chemicals, coal fly ash, and many others (Cozzarelli et al. 2016; Hajalilou et al. 2011; Mohan and Pittman, 2007; Orisakwe et al. 2004). According to Central Pollution Control Board (CPCB), the maximum industrial effluent discharge standard for As is 0.2 mg/ml, which is enough to cause health problems or even death for many species (Amadi et al. 2012; Okeyo et al. 2018). Short-term or continuous exposure to As can end up causing skin problems, fatigue, neurological disorders, lung disease, cardiovascular disease, and even death (Mohan and Pittman 2007). These severe effects urge the researchers to

Responsible Editor: George Z. Kyzas

✉ Biswajit Saha
sahab@nitrrkl.ac.in

¹ Department of Chemical Engineering, National Institute of Technology Rourkela (NIT Rourkela), Sector 1, Rourkela, Odisha 768009, India

² PRS-Nanoscience and Nanotechnology Centre, Department of Chemistry, D.S.B. Campus, Kumaun University, Nainital 263001, Uttarakhand, India

³ Centre for Nanomaterials, National Institute of Technology Rourkela (NIT Rourkela), Sector 1, Rourkela, Odisha 769008, India

develop a simple yet effective material and method for eliminating As ion from wastewater.

Many researchers have developed advanced methods for the purification of As from water bodies in recent years (Alka et al. 2021; Pandey et al. 2009; Weerasundara et al. 2021). Unfortunately, these methods are not economical or practical for large-scale treatment, and those processes produce secondary pollutants. Adsorption is the most efficient, economical and encouraging practice for the removal of pollutants from water (Ali and Gupta 2006; De Gisi et al. 2016). The materials used as an adsorbent play a vital role in this process; therefore, numerous materials, ranging from natural to exceptionally engineered materials, have already been explored as adsorbents. However, these adsorbents could not reach the expectation (John et al. 2018). Therefore, a simple yet effective and innovative alternative adsorbent has a high demand.

Ethylenediaminetetraacetic acid (EDTA) is widely known as a chelating and coordination agent for metal ions because of the formation of coordination complexes with the majority of metal ions with six ligands (Cui et al. 2015; Madadrang et al. 2012). This ability makes EDTA and its composite materials promising adsorbents for the removal of heavy metals. At the same time, the adsorption capacity of EDTA functionalised materials depends upon the property of base materials and the functional groups that anchor EDTA on the base material (Cui et al. 2015).

Recently, graphene and its composites have evolved as one of the most exciting materials in the research world. The large surface areas of graphene oxide (GO) and graphene derivatives are decorated with different functional groups, including hydroxyl, carboxyl, epoxide groups, etc. (Saha et al. 2018). These functional groups serve as more than merely active adsorption sites for various pollutants in aqueous solutions (Kyzas et al. 2015). Also, these functional groups can anchor other materials on the surface of GO to make different composite materials (Ranjan Rout and Mohan Jena, 2021; Saha et al. 2017; Verma et al. 2022). However, the separation of GO from the water media after use is problematic due to its high dispersion and tiny particle size. In this regard, magnetic nanoparticle-decorated GO could be an innovative solution. Iron (II, III) oxide (Fe_3O_4) nanoparticles are well known for their magnetic behaviour that facilitates easy separation of the adsorbent using an external magnet in real-field applications (Jabbar et al. 2022; Saha et al. 2018; Shen et al. 2009).

Fewer articles have reported the synthesis of amine-functionalisation with magnetic nanoparticles or graphene oxide-based nanocomposite and its applications in the adsorption of various heavy metals such as Pb(II), Cu(II), U(VI), Hg(II), Cd(II), Ni(II), Cr(VI), and As (III) (Einollahi Peer et al. 2018; Ghasemi et al. 2017; Liu et al. 2016; Shahzad et al. 2017; Sharif et al. 2019; Zhao et al.

2017). According to the acquired knowledge, this is the first study that has reported the adsorption of As(V) ions using EDTA@ Fe_3O_4 @GO nanocomposite. This work has adopted a simple pathway for the synthesis of EDTA functionalised magnetic graphene oxide (EDTA@ Fe_3O_4 @GO) nanocomposite and focused on the removal of deadly As(V) ions using the synthesised composite. Synthesised EDTA@ Fe_3O_4 @GO was analysed by Fourier transform infrared spectra (FTIR), X-ray diffraction (XRD), scanning electron microscope (SEM), Brunauer–Emmett–Teller (BET) and zeta potential. Furthermore, the adsorption process was investigated by the kinetic, isotherm, and thermodynamics characteristics to understand the efficiency and interaction mechanism between the EDTA@ Fe_3O_4 @GO and the targeted pollutant (As(V)). Also, the recycling ability of EDTA@ Fe_3O_4 @GO was studied to evaluate its economic benefits. The overall goal of this study is to develop a simple, efficient, and economical adsorbent for large-scale wastewater treatment.

Experimental work

Chemicals and reagents

Highly pure 100- μm -sized graphite flakes, sodium arsenate (Na_3AsO_4), iron (III) chloride hexahydrate ($\text{FeCl}_3 \cdot 6\text{H}_2\text{O}$) and methylene alcohol (CH_3OH) were purchased from Molychem, India. Other chemicals like sulphuric acid (H_2SO_4 , 98%), hydrogen peroxide (H_2O_2 , 30%) and phosphoric acid (H_3PO_4 , 75%) were purchased from Thermo Fisher Scientific India Pvt. Hydrochloric acid (HCl, 30%) and potassium permanganate (KMnO_4) were provided from Finar Limited. Various organic solvents such as ethanol and acetone were purchased from Sisco Research Laboratory. Ethylene glycol (EG), ammonia solution (NH_4OH) and sodium acetate ($\text{C}_2\text{H}_3\text{NaO}_2$) were bought from Merck. All the chemicals used in this study are highly pure and used with no additional purification. Deionised (DI) water was utilised for the entire experiment.

Synthesis of GO, Fe_3O_4 , Fe_3O_4 @GO and EDTA@ Fe_3O_4 @GO

The Improved hummers method was used to synthesise GO (Marcano et al. 2010). In this method, 1 g graphite powder and 6 g potassium permanganate were treated in an acid solution containing sulphuric acid and phosphoric acid in 1:9 ratios by volume. The mixture was stirred at 50 °C for 12 h. Later, the reaction was terminated by adding ice cubes and hydrogen peroxide. The synthesised product was washed with HCl, ethanol and water to eliminate unoxidised metal

ions. The washed GO was dried overnight at 60 °C before keeping it in a glass bottle for later use.

The Fe₃O₄ nanoparticles were synthesised by the hydrothermal method, which is mentioned elsewhere (Cao et al. 2015). In brief, 3 mmol of FeCl₃ and 10 mmol of urea were mixed with 20 ml of EG under contentious stirring conditions. The resultant solution was then allowed to react in a Teflon-lined stainless steel autoclave at 180 °C for 12 h. The autoclaved product was cleaned vigorously to eliminate undesirable particles. The washed Fe₃O₄ nanoparticles were subsequently dried overnight for future use. Furthermore, the GO and Fe₃O₄ nanoparticles were mixed in a 1:1 ratio and allowed to react at 180 °C in a Teflon-lined autoclave to synthesise Fe₃O₄@GO. The resultant product was then washed and dried overnight.

After that, 5 g of Fe₃O₄@GO nanocomposite was dispersed in 10% concentrated 100 ml acetic acid. Also, 30 g of EDTA was added to 100 ml methyl alcohol for EDTA dispersion. The dispersions were mixed and reacted at room temperature for 24 h to synthesise EDTA@Fe₃O₄@GO. The resultant product was cleaned, dried at 50 °C, and ground into a fine powder for further application.

Physiochemical characterisation

The surface structure of the EDTA@Fe₃O₄@GO was analysed by a scanning electron microscope (JEOL JSM-6480). Chemical compositions and the active bond types were investigated using FTIR spectroscopy (Nicolet Is10, Thermo Fisher, 2007). The diffraction peaks obtained from the XRD analyser (D8 Advance Bruker instrument) were used to examine the phase and crystallography of the synthesised material. Defects on carbon lattice were analysed using Raman spectroscopy analysis (model- XMB3000-3000). The specific surface area was evaluated from the N₂ adsorption–desorption isotherm (ASAP 2000 surface area analyser). Malvern zeta meter (Zeta sizer 2000, UK) was used to measure the Zeta potential at different pH ranges. UV spectroscopy (Jasco, Model V-530, Japan) was used to measure the concentration of pollutants in an aqueous solution at 345 nm wavelength.

Adsorption study

The adsorption behaviour of As(V) ion onto EDTA@Fe₃O₄@GO nanocomposite was studied in the batch adsorption experiment. In this study, sodium arsenate was used as a source of As(V) ions. The adsorption behaviour of As(V) on EDTA@Fe₃O₄@GO was investigated under different conditions. The concentrations of the adsorbate before and after the adsorption were measured by a UV–Visible spectrophotometer. Other adsorption conditions were optimised for kinetic, isotherm and

thermodynamics studies. The percentage removal (%R), equilibrium adsorption capacity (q_e) and adsorption capacity at time t (q_t) were calculated from Eqs. 1, 2 and 3, respectively:

$$\%R = \frac{(C_o - C_t)}{C_o} \times 100 \quad (1)$$

$$q_e = (C_o - C_e) \times \frac{V}{w} \quad (2)$$

$$q_t = (C_o - C_t) \times \frac{V}{w} \quad (3)$$

where C_o , C_e and C_t represent the initial concentration of As(V) (mg/L), the concentration of As(V) at the equilibrium stage and the concentration of As(V) at time t , respectively. w is the amount of EDTA@Fe₃O₄@GO (mg), and V is the volume of pollutant solution (ml).

Regeneration and recycling

Regeneration and recycling of adsorbents are critical from economic and environmental standpoints. Fifty millilitres of HCl solution with different concentration (0.1–1 mol/L) was mixed with pollutant-loaded EDTA@Fe₃O₄@GO and sonicated for 30 min to regenerate the adsorbent. Then, the adsorbent material was separated, washed with DI water and dried for recycling. The recovered As(V) ion was determined by UV-spectroscopy.

Error analysis

Error analysis is another aspect of the determination of the best fit model for the adsorption process. Two error functions, average relative error (ARE) and root mean square error (RMSE), were employed to measure the coherence between experimental data and calculated values derived by models (Terdtuttakun et al. 2017), as shown in Eqs. 4 and 5, respectively:

$$ARE = \frac{100}{n} \sum_{i=1}^n \left| \frac{q_{e,meas} - q_{e,calc}}{q_{e,meas}} \right| \quad (4)$$

$$RMSE = \sqrt{\frac{1}{n} \sum_{i=1}^n (q_{e,exp} - q_{e,cal})_i^2} \quad (5)$$

where $q_{e,exp}$ and $q_{e,cal}$ are the adsorbed quantities determined by the experiment and the adsorption isotherm model, respectively. n is the number of data points.

Results and discussion

Characterisation of EDTA@Fe₃O₄@GO nanocomposite

Structural and morphological analyses Various morphological analyses were performed to develop an overall understanding of the material and its structural properties. At first, high-resolution micro-level images (Fig. 1) were taken using a scanning electron microscope (SEM) to investigate the surface morphology of the synthesised nanocomposite. The SEM image in Fig. 1 shows that the EDTA@Fe₃O₄ particles are uniformly distributed on the wrinkled and folded GO sheets.

Analysis of functional groups Furthermore, various bonds and functional groups present in EDTA@Fe₃O₄@GO were studied by the FTIR analysis. Comparative results of FTIR spectra taken from GO, Fe₃O₄@GO and EDTA@Fe₃O₄@GO are shown in Fig. 2. FTIR spectra of GO show four peaks located at 1755, 1580, 1248 and 1013 cm⁻¹, corresponding to four primary bands of GO, such as C=O, C=C, CO-H and C-O-C, respectively, which confirms the successful oxidation of graphite according to previously stated studies (Bera et al. 2018). However, the intensity of the GO peaks decreases in the FTIR spectrum of Fe₃O₄@GO. In addition, a peak is observed at around 610 cm⁻¹, corresponding to the Fe-O vibrational mode of Fe₃O₄ (Raghu et al. 2017). The FTIR spectrum of EDTA@Fe₃O₄@GO shows peaks at 3434, 2985, 1725, 1481, 1382, 1223 and 623 cm⁻¹ corresponding to O-H, N-H, C=O, C-N, C-OH, C-NH₂ and Fe-O, respectively. Compared to GO and Fe₃O₄@GO, EDTA@Fe₃O₄@GO has maximum oxygen and nitrogen-containing

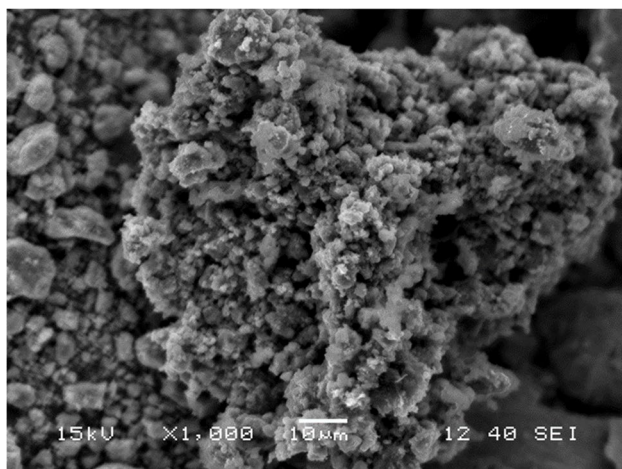


Fig. 1 SEM image of EDTA@Fe₃O₄@GO

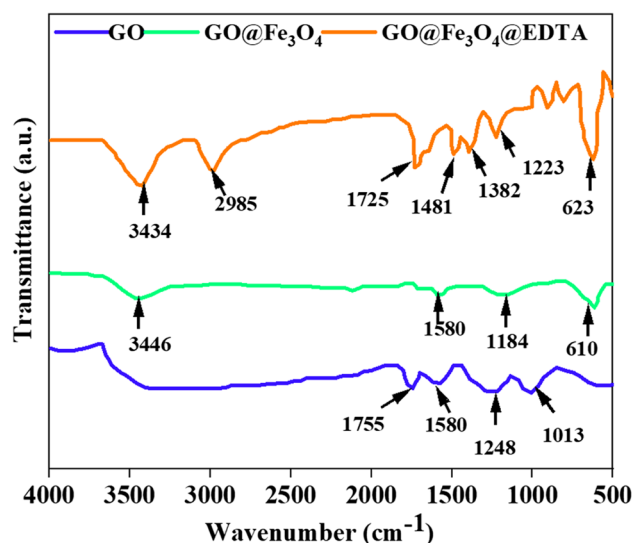


Fig. 2 FTIR analysis of Fe₃O₄@GO and EDTA@Fe₃O₄@GO

functional groups, which are the primary reactive sites of this composite for the adsorption of heavy metals.

Structural analysis The crystallinity of GO, Fe₃O₄@GO and EDTA@Fe₃O₄@GO was analysed by the XRD spectra, as shown in Fig. 3. EDTA@Fe₃O₄@GO nanocomposite shows the diffraction peaks at $2\theta = 28.37^\circ, 35.6^\circ, 46^\circ, 61^\circ, 65.8^\circ$ and 73.7° corresponding to the (220), (311), (400), (422), (511) and (440) lattice planes of Fe₃O₄, respectively (Cui et al. 2015). This observation advocates for the presence of Fe₃O₄ nanoparticles in the EDTA@Fe₃O₄@GO nanocomposite in a large quantity. The characteristic XRD peak of GO that appeared at 11.8° supports the successful synthesis of materials (Guo and Bulin, 2021).

Analysis of surface area The surface area of an adsorbent is a crucial parameter in the adsorption process as the adsorption capacity is directly proportional to the surface area (John et al. 2018). N₂ adsorption-desorption isotherm analysis has been performed to analyse the surface area of prepared nanocomposites (Zhou et al. 2009). The Brunauer-Emmett-Teller (BET) analysis measured through the N₂ adsorption-desorption isotherm process shows that EDTA@Fe₃O₄@GO has a surface area of about 52.32 m²/g (Fig. 4a). The obtained adsorption-desorption graph follows the type-IV hysteresis loop (Cui et al. 2015), indicating the conical structure with many side holes due to the gaps between EDTA-nanoparticles and GO sheets. Furthermore, the pore size analysis by Barrett-Joyner-Halenda (BJH) pore size distribution shows a sharp peak at around 16 nm in Fig. 4b. The surface properties such as mesoporous structure, large surface area and abundant active sites on EDTA@Fe₃O₄@GO make this material an excellent adsorbent (Zhou et al. 2009).

Fig. 3 XRD analysis of $\text{Fe}_3\text{O}_4@$ GO and $\text{EDTA}@$ $\text{Fe}_3\text{O}_4@$ GO

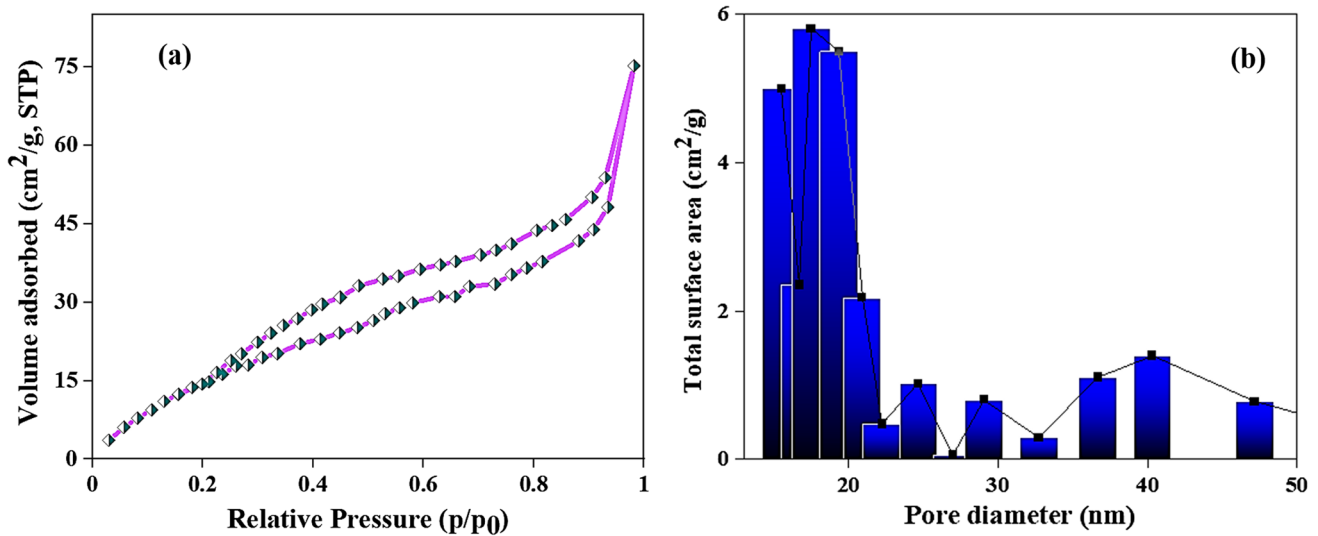
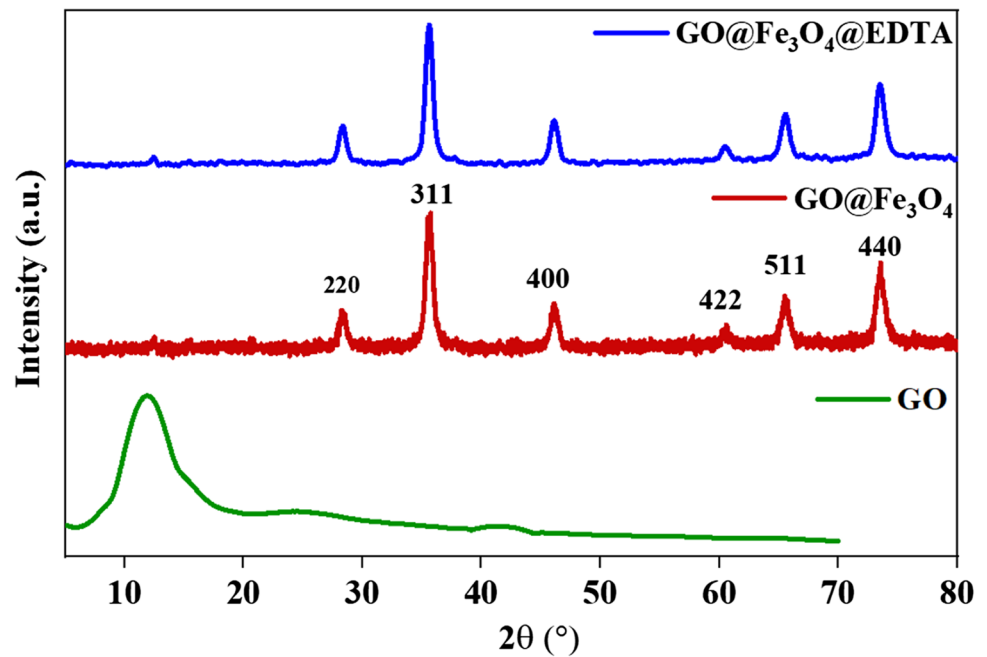


Fig. 4 **a** BET analysis of $\text{EDTA}@$ $\text{Fe}_3\text{O}_4@$ GO, **b** pore size distribution of $\text{EDTA}@$ $\text{Fe}_3\text{O}_4@$ GO

Analysis of surface charge Zeta potential is an essential tool for analysing the overall surface charge and electrophoretic mobility of the particles. Figure 5 shows the zeta potential of the $\text{EDTA}@$ $\text{Fe}_3\text{O}_4@$ GO measured at various pHs starting from 1 to 10. The pH of zero point of charge (pH_{zpc}) is 2.36, and the surface of the $\text{EDTA}@$ $\text{Fe}_3\text{O}_4@$ GO is negatively charged at a pH greater than 2. Based on these findings, it is possible to assume that the synthesised $\text{EDTA}@$ $\text{Fe}_3\text{O}_4@$ GO would be negatively charged in most regular water environments as the pH of regular water typically ranges between 6 and 9 (Moussavi and Barikbin, 2010). The zeta potential of

the $\text{EDTA}@$ $\text{Fe}_3\text{O}_4@$ GO shifts toward the negative region with the increase in pH, which promotes the sorption capacities of cation pollutants in aquatic environments.

The adsorption deciding factors

Effect of pH on adsorption capacity

Solution pH has a significant impact on the adsorption capacity of the adsorbent. The solution pH influences the charge transfer between pollutant particles and adsorbents in

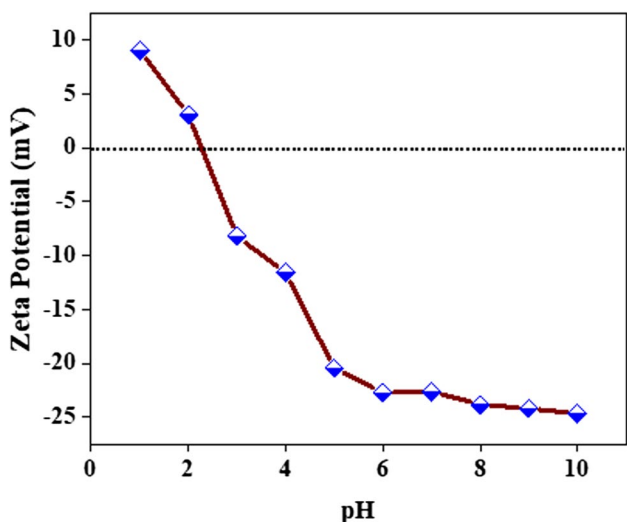
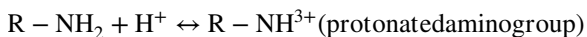


Fig. 5 Zeta potential analysis of EDTA@Fe₃O₄@GO

an aqueous solution (Zhou et al. 2011). Figure 6 shows the effect of pH (2 to 12) on the percentage removal of As(V) using EDTA@Fe₃O₄@GO nanocomposite. The experimental results show that the percentage removal of As(V) using EDTA@Fe₃O₄@GO nanocomposite is maximum at low pH. The chelating groups present in the composite play a vital role in this characteristic. The possible reason behind the maximum percentage removal in an acidic medium is the presence of a large number of H⁺ ions, which protonate the amino groups (–NH₂) of EDTA@Fe₃O₄@GO.



As per the results obtained from zeta potential, it was clear that the overall surface charge of EDTA@Fe₃O₄@GO would

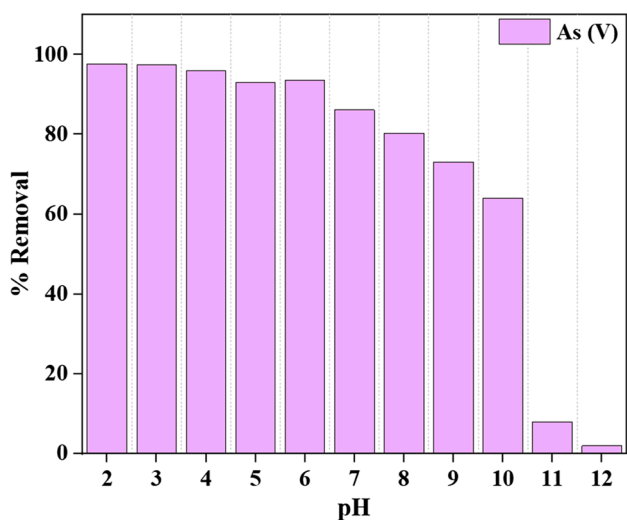


Fig. 6 The influence of solution pH on percentage removal of As(V)

be positive below pH 2. As(V) is a negatively charged ion; therefore, the electrostatic force allows the binding of As(V) ions on the surface of positively charged EDTA@Fe₃O₄@GO.

Effect of adsorbent amount on percentage removal

The effect of adsorbent amount on adsorption capacity was examined by adding EDTA@Fe₃O₄@GO nanocomposite from 5 to 25 mg in 50 ml of As(V) solutions. Figure 7 summarises the influence of EDTA@Fe₃O₄@GO amounts on adsorption behaviour. The findings show the removal efficiency increases with an increase in adsorbent amount, and it reaches 99% for an adsorbent amount of 20 mg. The removal efficiency increases due to the rise in active adsorption sites, which is directly proportional to the adsorbent amount (Mousavi and Barikbin, 2010) (Bansal et al. 2009). However, the removal percentage does not improve after a further rising in the adsorbent amount to 25 mg. The above results suggest that 20 mg of EDTA@Fe₃O₄@GO is the saturation amount of the adsorbent for the given As(V) solution.

Adsorption kinetics

Adsorption mechanism and adsorption capacity were studied using pseudo-first-order (PFO) and pseudo-second-order (PSO) kinetic models. The acquired experimental data were fitted to the kinetics models to investigate the adsorption kinetics. Equations 6 and 7 express the nonlinear forms of PFO and PSO kinetic models, respectively:

$$q_t = q_e(1 - e^{-k_1 t}) \tag{6}$$

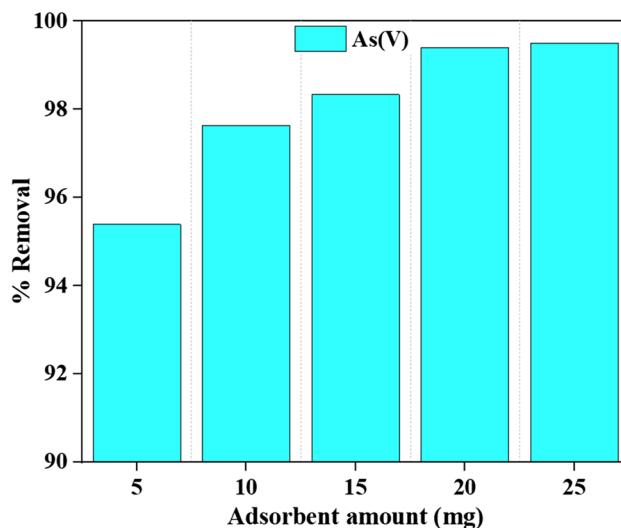


Fig. 7 Effect of adsorbent amount on percentage removal of As(V)

$$q_t = \left(\frac{q_e^2 k_2 t}{1 + q_e k_2 t} \right) \tag{7}$$

where K_1 and K_2 are the rate constant of the PFO and PSO kinetic models, respectively. q_e and q_t represent the adsorption capacity at equilibrium and at time t , respectively, and t represents the time.

The curvatures fitted with the PFO kinetic model have the correlation coefficients (R^2) of 0.937, 0.941, 0.943 and 0.944 for 50, 100, 150 and 200 mg/L solutions, respectively. In comparison, the R^2 values for curvatures fitted with the PSO kinetic model for all samples are approximately 1 ($R^2 \sim 0.99$), and the experimental values are also in accordance with the calculated values. The findings from fitted kinetic curves are depicted in Fig. 8 and presented in Table 1, which conclude that the As(V) ion adsorption onto EDTA@Fe₃O₄@GO nanocomposite obeys the PSO kinetic model. Furthermore, the findings imply that the adsorption rate is mainly determined by surface complexation (Aydin and Aksoy 2009).

Adsorption isotherms

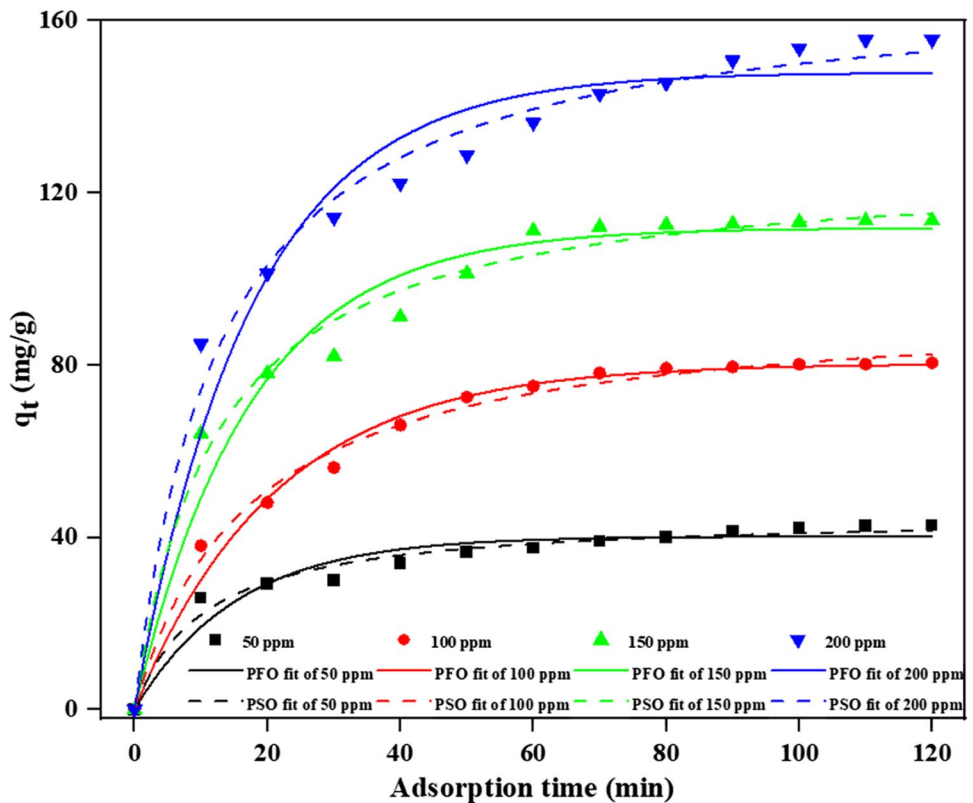
Adsorption isotherms were investigated to understand the adsorption mechanism and optimum adsorption capacity of the EDTA@Fe₃O₄@GO nanocomposite. Here, adsorption

Table 1 Various parameters obtained from the kinetic models

Parameters/(ppm)	50	100	150	200
q_{exp} (mg/g)	42.808	80.521	113.558	155.6
Pseudo first order				
k_1 (min ⁻¹)	0.931	0.952	0.959	0.954
q_{cal} (mg/g)	30.236	65.124	104.858	141.017
R^2	0.937	0.941	0.943	0.944
ARE (%)	27.03	19.45	7.98	9.34
RMSE	7.25	8.89	5.15	8.42
Pseudo second order				
$k_2 \times 10^3$ (g/mg min)	2.09	0.624	0.65	0.46
q_{cal} (mg/g)	45.272	85.451	118.785	162.421
R^2	0.981	0.991	0.989	0.988
ARE (%)	5.75	6.122	4.66	4.38
RMSE	1.45	2.84	2.97	3.45

isotherms were analysed by using the Langmuir isotherm model (LIM), Freundlich isotherm model (FIM) and Temkin isotherm model (TIM). The LIM proclaims unilayer adsorption, whereas the FIM proclaims multilayer adsorption and surface heterogeneity. In contrast, the TIM deals with the interaction of adsorbate and adsorbent in terms of binding energy. According to this model, the heat of adsorption decreases linearly as the adsorbent surface is covered (Wang

Fig. 8 Experimental data fitted with PFO and PSO kinetic models



and Guo 2020). The nonlinear expression for LIM, FIM and TIM is expressed as Eqs. 8, 9 and 10, respectively:

$$q_e = \frac{q_t K_L C_e}{1 + K_L C_e} \quad (8)$$

$$q_e = K_F (C_e)^{1/n} \quad (9)$$

$$q_e = B_T \ln(A_T) + B_T \ln(C_e) \quad (10)$$

where C_e is the concentration at equilibrium, q_e is the equilibrium adsorption capacity and q_t adsorption capacity at a given time t . K_L is the Langmuir adsorption constant (L/mg) correlated to the heat of adsorption, q_m is the maximal adsorption capacity of the adsorbent (mg/g). K_F and n represent the Freundlich isotherm constant indicating relative adsorption energy and adsorption intensity. Here, $B_T = RT/b$, where b represents the Temkin constant, related to the heat of adsorption (Jmol^{-1}), and A_T represents the binding energy (Lg^{-1}).

Experimental results of equilibrium adsorption were fitted to LIM, FIM and TIM, as shown in Fig. 9. Obtained parameters from the fitted models are given in Table 2. Results show that the FIM is the best-fitted model for the removal of As(V) by $\text{EDTA@Fe}_3\text{O}_4\text{/GO}$ nanocomposite at given conditions. The value of n confirms the favourability

Table 2 Obtained isotherm parameters from different isotherm models

Isotherm models	Parameters	Value
Langmuir	q_m (mg/g)	178.214
	K_L (L/mg)	0.121
	R^2	0.948
	R^2_{adj}	0.935
Freundlich	K_F (mg/g) (L/mg) ^{1/n}	225.214
	n	0.241
	R^2	0.996
	R^2_{adj}	0.995
Temkin	b (J/mol)	42.82
	A_T (L/mg)	2.452
	R^2	0.981
	R^2_{adj}	0.978

of the adsorption process as its value (0.241) lies between 0 and 1.

Thermodynamics study

In the adsorption study, the thermodynamics investigation is important to understand the thermal behaviour of this process. Various thermodynamics parameters like change in entropy (ΔS°), enthalpy (ΔH°) and Gibbs free energy (ΔG°) were analysed using the following equations:

Fig. 9 Various isotherm models fitted to experimental data

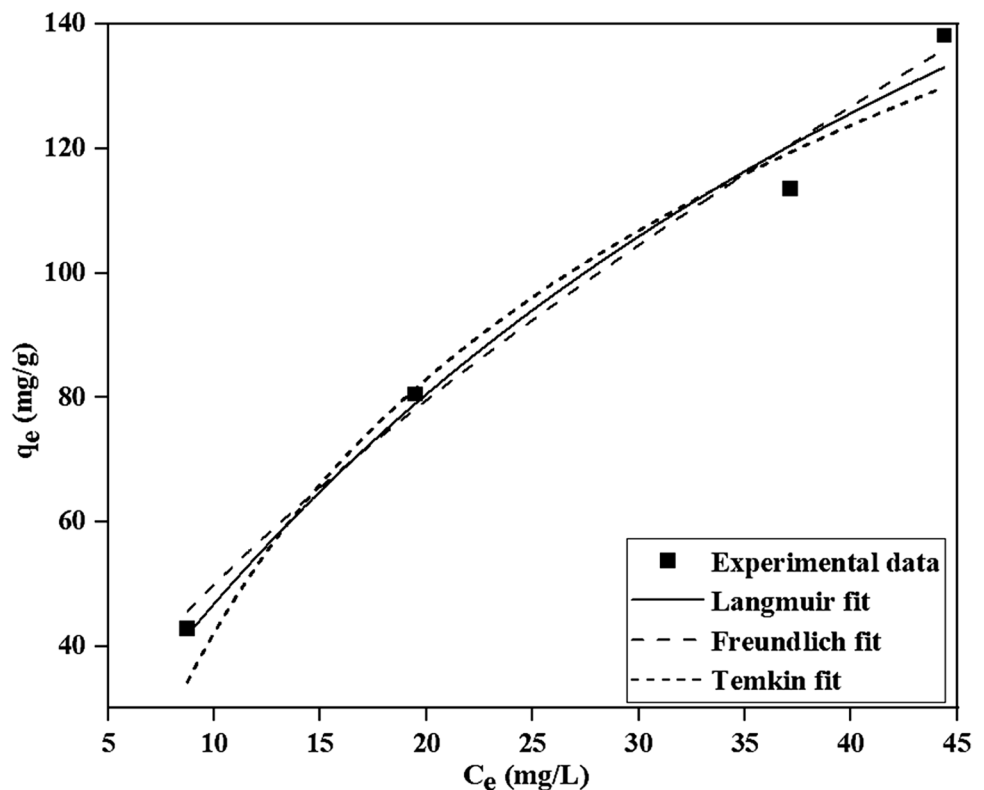


Table 3 Different parameters obtained from thermodynamics study

Temperature (K)	ΔG° (kJ/mol)	ΔH° (kJ/mol)	ΔS° (J/mol K)
293	-13.47	43.674	195.046
298	-14.45		
303	-15.42		
308	-16.40		
313	-17.37		

$$\ln(\rho K_d) = \frac{\Delta S^0}{R} - \frac{\Delta H^0}{RT} \tag{11}$$

$$K_d = \frac{q_e}{C_e} \tag{12}$$

$$\Delta G^\circ = \Delta H^\circ - T\Delta S^\circ \tag{13}$$

where ρ is the density (g/L), K_d is the adsorption coefficient (L/g), R is the universal gas constant (8.314 J/mol K), and T

is the temperature (°K). C_e and q_e represent the equilibrium concentration of As(V) and equilibrium adsorption capacity of the composite, respectively. The slope and intercept of the plot of $\ln(\rho K_d)$ vs. $1/T$ were used to calculate ΔH° and ΔS° . Table 3 shows the calculated thermodynamics parameters. The negative value of ΔG° at high temperature confirms that the adsorption of As(V) onto EDTA@Fe₃O₄@GO is spontaneous. Furthermore, the endothermic nature of the adsorption process was supported by the positive value of ΔH° calculated from Van't Hoff plot (Fig. 10). The positive values of ΔS° during the adsorption of As(V) onto EDTA@Fe₃O₄@GO reflect an increase in randomness at the solid–liquid interface (Singh and Pant 2004).

Regeneration study

The adsorbed As(V) was recovered, and EDTA@Fe₃O₄@GO was regenerated using an HCl solution. In order to get the optimum desorption of As(V), the effect of differently concentrated HCl solutions on the desorption of As(V) was examined and is presented in Table 4. The results

Fig. 10 Thermodynamics study for the adsorption of As(V)

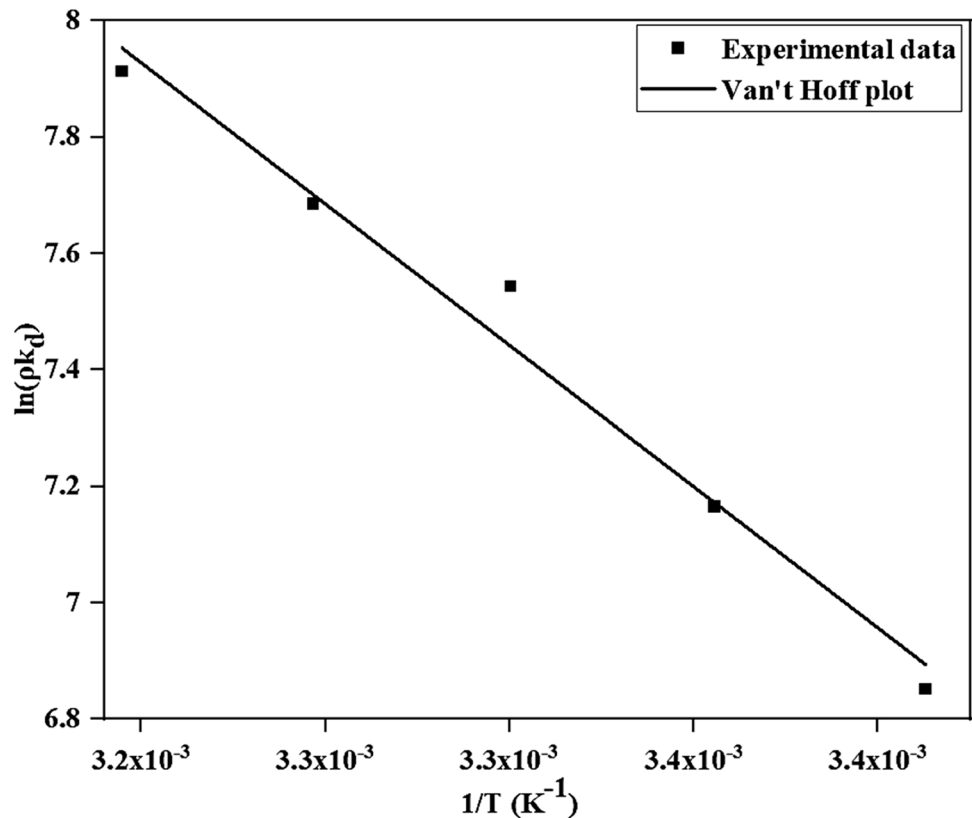


Table 4 Effect of HCl concentration on percentage desorption of As(V)

Concentration of HCl (mol/L)	0.1	0.2	0.3	0.4	0.5	0.6	0.7	0.8	0.9	1
% Desorption	27.65	46.69	70.18	88.45	95.06	95.32	95.55	95.61	95.77	95.8

show that the desorption efficiency is higher at concentrated HCl solutions. As mentioned earlier, the surface of $\text{EDTA@Fe}_3\text{O}_4\text{@GO}$ would be protonated in the acetic environment; hence, the coordination between the metal ions and active sites of $\text{EDTA@Fe}_3\text{O}_4\text{@GO}$ nanoparticles might be reduced. Recycle experiment was preferred at 0.5 mol/L of HCl solution for desorption of heavy metal as the strong acid environment induces the decomposition of adsorbents. The recyclability study (Fig. 11) reveals that $\text{EDTA@Fe}_3\text{O}_4\text{@GO}$ has good removal efficiency (~68%) even after the 5th cycle. The excellent recyclability of this material makes it an efficient and economical adsorbent.

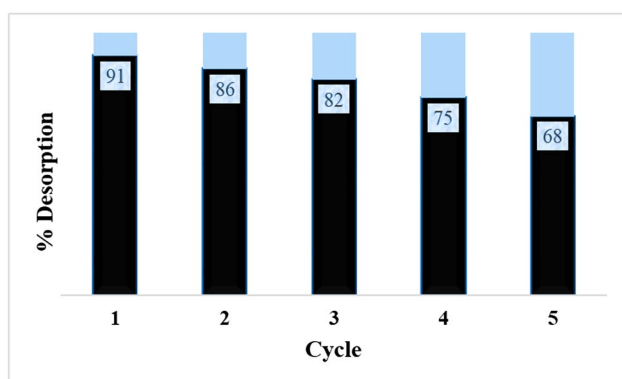
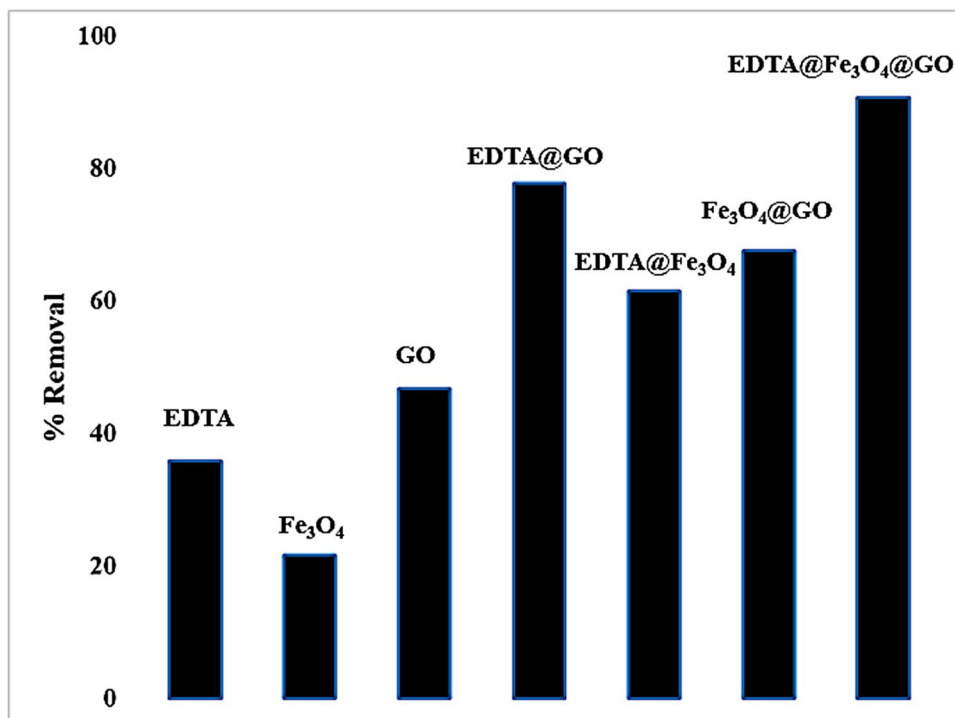


Fig. 11 Recycle study of $\text{EDTA@Fe}_3\text{O}_4\text{@GO}$ for the adsorption of As(V)

Fig. 12 A comparative analysis of the % removal of As(V) using different materials



Comparative analysis

Here, the performance of the synthesised $\text{EDTA@Fe}_3\text{O}_4\text{@GO}$ nanocomposite is composed of GO, Fe_3O_4 and EDTA. Each of these adsorbents has its specific ability to remove heavy metals due to their particular structural properties and characteristics. As shown in Fig. 12, the As(V) removal efficiency of $\text{EDTA@Fe}_3\text{O}_4\text{@GO}$ is about 90.15%, whereas As(V) removal efficiency of mono-component (EDTA, GO and Fe_3O_4) and bi-component ($\text{EDTA@Fe}_3\text{O}_4$, $\text{Fe}_3\text{O}_4\text{@GO}$ and EDTA@GO) are below 50% and 80%, respectively. This analysis confirmed that the $\text{EDTA@Fe}_3\text{O}_4\text{@GO}$ nanocomposite is an effective adsorbent for the removal of As(V) aqueous medium.

Adsorption mechanism and performance evaluation

Comparative analysis (Fig. 12) has found that EDTA@GO shows better adsorption performance than $\text{EDTA@Fe}_3\text{O}_4$, $\text{Fe}_3\text{O}_4\text{@GO}$, GO and Fe_3O_4 nanoparticles. EDTA and GO played a vital role in removing As(V) ions. The ethylenediaminetetraacetic acid radical (Y^{4-}) present in EDTA is a hexadentate ligand with a strong coordination ability that forms the material coordinate with heavy metal ions. This coordination interaction between As(V) ions and EDTA is one of the reasons behind the excellent adsorption of As(V) onto $\text{EDTA@Fe}_3\text{O}_4\text{@GO}$. Apart from the coordination interaction, the electrostatic attraction among oxygen-containing functional groups present on the GO surface and As(V) ions is another reason behind the high adsorption capacity of the

EDTA@Fe₃O₄@GO nanocomposite (Fig. 13) (Guo et al. 2014; Sun et al. 2012). Due to this coordination and electrostatic interaction, EDTA@Fe₃O₄@GO showed outstanding adsorption capacity towards As(V) ions.

Furthermore, a comparative As(V) adsorption study was conducted between EDTA@Fe₃O₄@GO nanocomposite and various other adsorbents (Table 5). The high adsorption capacity of EDTA@Fe₃O₄@GO compared to other adsorbents validates its exceptional adsorption performance. The simplicity of the synthesis method and excellent removal capacity of EDTA@Fe₃O₄@GO can lead this material to a broad application.

Conclusion

In the present work, highly efficient and multifunctional EDTA functionalised magnetite graphene oxide was synthesised via a facile method to remove As(V) ion. The EDTA@Fe₃O₄@GO nanocomposite showed a very high adsorption capacity for As(V) after introducing amine groups on the surface of Fe₃O₄@GO. In an acidic medium (pH < 2), the adsorption capacity was found to be maximum due to the possible protonation of amine groups (–NH₂) in the presence of H⁺ ions. The removal mechanism is mainly attributed to the electrostatic attraction between As(V) and EDTA@Fe₃O₄@GO. Based on the results of kinetic and isotherm investigations, it is possible to conclude that the adsorption process follows the PSO kinetic model and the FIM.

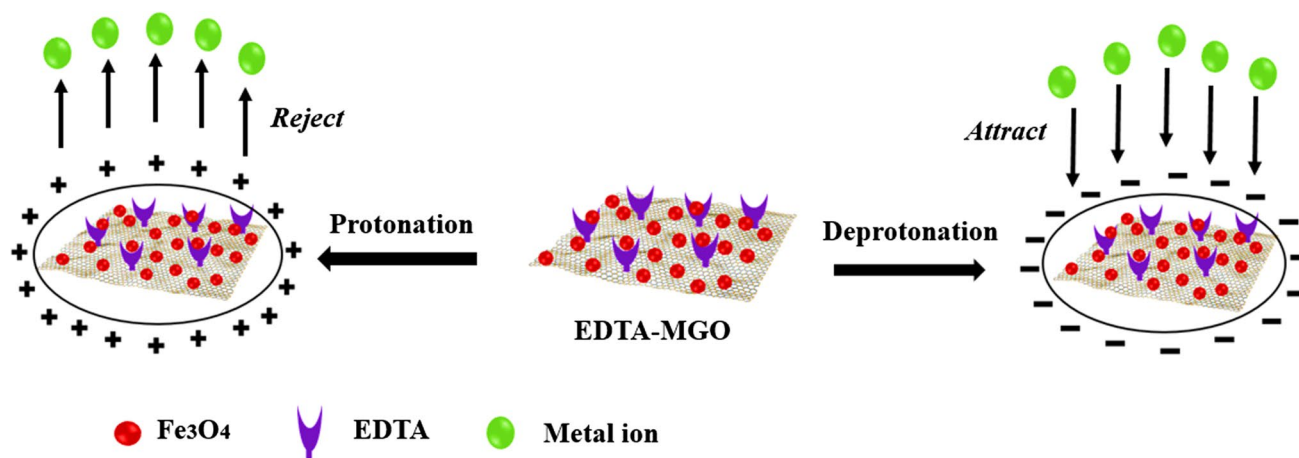


Fig. 13 Mechanism behind the adsorption phenomena of EDTA@Fe₃O₄@GO

Table 5 Performance evaluation of different adsorbents for the removal of As(V)

Adsorbent	Pollutant	Adsorption capacity (mg/g)	Reference
EDTA-GO	Pb(II)	479	Madadrang et al. (2012)
GO-ethylene diamine triacetic acid	Cu(II)	108	Mejias Carpio et al. (2014)
Al ₂ O ₃ -iron oxide composite	Pb(II)	28.98	Huang et al. (2007)
Chitosan sphere	Hg(II)	31	Vieira and Beppu (2006)
γ-Fe ₂ O ₃ -carbonaceous materials	Pb(II)	20	Ohno et al. (2011)
Magnetic ionic liquid-chitosan-GO	Cr(VI)	143.5	Li et al. (2014)
CoFe ₂ O ₄ -carbon nanotubes	Pb(II)	57	Zhou et al. (2014)
Graphene oxide nanosheet	U(VI)	97	Zhao et al. (2011)
Chitosan-coated bentonite beads	Cu(II)	12	Dalida et al. (2011)
Amino functionalised magnetic graphene oxide (AMGO)	U(VI)	141	Chen et al. (2016)
Cation-exchange resin-supported polyethyleneimine	Cu(II)	200	Chen et al. (2010)
GO/PPy composites	U(VI)	147	Liu et al. (2014)
EDTA@Fe ₃ O ₄ @GO	As(V)	178.214	This study

The EDTA@Fe₃O₄@GO has a maximum As(V) adsorption capacity of 178.214 mg/g, which is higher than GO and Fe₃O₄@GO. The thermodynamics data ($\Delta G^\circ < 0$, $\Delta H^\circ > 0$, $\Delta S^\circ > 0$) suggested that the adsorption of As(V) ion onto EDTA@Fe₃O₄@GO nanocomposite is an endothermic and spontaneous process. High adsorbent capacity, excellent recyclability and easy reproducibility make the EDTA@Fe₃O₄@GO nanocomposite an economical and efficient adsorbent for the removal of heavy metals from wastewater.

Author contribution All the authors contributed to the study's conception and design. Material preparation, data collection and analysis were performed by Prateekshya Suman Sahu and Ravi Prakash Verma. Prateekshya Suman Sahu wrote the first draft of the manuscript, and Nanda Gopal Sahoo and Chetna Tewari commented on the previous version of the manuscript. Dr. Biswajit Saha has supervised the work and read and approved the final manuscript.

Funding This research was supported by the "Science and Engineering Research Board (by the Government of India) (ECR/2018/001192 and EEQ/2018/000509)". The authors also acknowledge the financial grant received from the Department of Science and Technology (DST), Government of India, Grant number DST/TM/WTI/WIC/2K17/82(G).

Data availability Not applicable.

Declarations

Ethics approval and consent to participate Not applicable.

Consent for publication Not applicable.

Competing interests The authors declare no competing interests.

References

- Ali I, Gupta VK (2006) Advances in water treatment by adsorption technology. *Nat Protoc* 1:2661–2667. <https://doi.org/10.1038/nprot.2006.370>
- Alka S, Shahir S, Ibrahim N, Ndejiko MJ, Vo D-VN, Manan FA (2021) Arsenic removal technologies and future trends: a mini review. *J Clean Prod* 278:123805. <https://doi.org/10.1016/j.jclepro.2020.123805>
- Amadi AN, Yisa J, Ogbonnaya IC, Dan-Hassan MA, Jacob JO, Alkali YB (2012) Quality evaluation of river chanchaga using metal pollution index and principal component analysis. *J Geogr Geol* 4. <https://doi.org/10.5539/jgg.v4n2p13>
- Aydın YA, Aksoy ND (2009) Adsorption of chromium on chitosan: optimization, kinetics and thermodynamics. *Chem Eng J* 151:188–194. <https://doi.org/10.1016/j.cej.2009.02.010>
- Bansal M, Singh D, Garg VK (2009) A comparative study for the removal of hexavalent chromium from aqueous solution by agriculture wastes' carbons. *J Hazard Mater* 171:83–92. <https://doi.org/10.1016/j.jhazmat.2009.05.124>
- Bera M, Gupta CP, Maji PK (2018) Facile one-pot synthesis of graphene oxide by sonication assisted mechanochemical approach and its surface chemistry. *J Nanosci Nanotechnol* 18:902–912. <https://doi.org/10.1166/jnn.2018.14306>
- Cao W, Ma Y, Zhou W, Guo L (2015) One-pot hydrothermal synthesis of rGO-Fe₃O₄ hybrid nanocomposite for removal of Pb(II) via magnetic separation. *Chem Res Chinese Univ* 31:508–513. <https://doi.org/10.1007/s40242-015-4487-6>
- Chen L, Zhao D, Chen S, Wang X, Chen C (2016) One-step fabrication of amino functionalized magnetic graphene oxide composite for uranium(VI) removal. *J Colloid Interface Sci* 472:99–107. <https://doi.org/10.1016/j.jcis.2016.03.044>
- Chen Y, Pan B, Li H, Zhang W, Lv L, Wu J (2010) Selective removal of Cu(II) ions by using cation-exchange resin-supported polyethyleneimine (PEI) nanoclusters. *Environ Sci Technol* 44:3508–3513. <https://doi.org/10.1021/es100341x>
- Cozzarelli IM, Schreiber ME, Erickson ML, Ziegler BA (2016) Arsenic cycling in hydrocarbon plumes: secondary effects of natural attenuation. *Groundwater* 54:35–45. <https://doi.org/10.1111/gwat.12316>
- Cui L, Wang Y, Gao L, Hu L, Yan L, Wei Q, Du B (2015) EDTA functionalized magnetic graphene oxide for removal of Pb(II), Hg(II) and Cu(II) in water treatment: adsorption mechanism and separation property. *Chem Eng J* 281:1–10. <https://doi.org/10.1016/j.cej.2015.06.043>
- Dalida MLP, Mariano AFV, Futralan CM, Kan C-C, Tsai W-C, Wan M-W (2011) Adsorptive removal of Cu(II) from aqueous solutions using non-crosslinked and crosslinked chitosan-coated bentonite beads. *Desalination* 275:154–159. <https://doi.org/10.1016/j.desal.2011.02.051>
- De Gisi S, Lofrano G, Grassi M, Notarnicola M (2016) Characteristics and adsorption capacities of low-cost sorbents for wastewater treatment: a review. *Sustain Mater Technol* 9:10–40. <https://doi.org/10.1016/j.susmat.2016.06.002>
- Einollahi Peer F, Bahramifar N, Younesi H (2018) Removal of Cd (II), Pb (II) and Cu (II) ions from aqueous solution by polyamidoamine dendrimer grafted magnetic graphene oxide nanosheets. *J Taiwan Inst Chem Eng* 87:225–240. <https://doi.org/10.1016/j.jtice.2018.03.039>
- Ezzeddine Z, Batonneau-Gener I, Pouilloux Y, Hamad H, Saad Z, Kazpard V (2015) Divalent heavy metals adsorption onto different types of EDTA-modified mesoporous materials: effectiveness and complexation rate. *Microporous Mesoporous Mater* 212:125–136. <https://doi.org/10.1016/j.micromeso.2015.03.013>
- Ghasemi E, Heydari A, Sillanpää M (2017) Superparamagnetic Fe₃O₄@EDTA nanoparticles as an efficient adsorbent for simultaneous removal of Ag(I), Hg(II), Mn(II), Zn(II), Pb(II) and Cd(II) from water and soil environmental samples. *Microchem J* 131:51–56. <https://doi.org/10.1016/j.microc.2016.11.011>
- Guo T, Bulin C (2021) Facile preparation of MgO/graphene oxide nanocomposite for efficient removal of aqueous Congo red: adsorption performance and interaction mechanism. *Res Chem Intermed* 47:945–971. <https://doi.org/10.1007/s11164-020-04310-9>
- Guo X, Du B, Wei Q, Yang J, Hu L, Yan L, Xu W (2014) Synthesis of amino functionalized magnetic graphenes composite material and its application to remove Cr(VI), Pb(II), Hg(II), Cd(II) and Ni(II) from contaminated water. *J Hazard Mater* 278:211–220. <https://doi.org/10.1016/j.jhazmat.2014.05.075>
- Hajalilou B, Mosaferi M, Khaleghi F, Jadidi S, Vosugh B, Fatehifar E (2011) Effects of abandoned arsenic mine on water resources pollution in north west of iran. *Heal Promot Perspect* 1:62–70. <https://doi.org/10.5681/hpp.2011.006>
- Huang Y-H, Hsueh C-L, Huang C-P, Su L-C, Chen C-Y (2007) Adsorption thermodynamic and kinetic studies of Pb(II) removal from water onto a versatile Al₂O₃-supported iron oxide. *Sep Purif Technol* 55:23–29. <https://doi.org/10.1016/j.seppur.2006.10.023>
- Jabbar KQ, Barzinjy AA, Hamad SM (2022) Iron oxide nanoparticles: preparation methods, functions, adsorption and coagulation/flocculation in wastewater treatment. *Environ Nanotechnology, Monit Manag* 17:100661. <https://doi.org/10.1016/j.enmm.2022.100661>

- John Y, David VE, Mmereki D (2018) A comparative study on removal of hazardous anions from water by adsorption: a review. *Int J Chem Eng* 2018:1–21. <https://doi.org/10.1155/2018/3975948>
- Khan K, Lu Y, Khan H, Zakir S, Khan IS, Khan AA, Wei L, Wang T (2013) Health risks associated with heavy metals in the drinking water of Swat, northern Pakistan. *J. Environ. Sci.* 25:2003–2013. [https://doi.org/10.1016/S1001-0742\(12\)60275-7](https://doi.org/10.1016/S1001-0742(12)60275-7)
- Kyzas GZ, Koltsakidou A, Nanaki SG, Bikiaris DN, Lambropoulou DA (2015) Removal of beta-blockers from aqueous media by adsorption onto graphene oxide. *Sci Total Environ* 537:411–420. <https://doi.org/10.1016/j.scitotenv.2015.07.144>
- Li L, Luo C, Li X, Duan H, Wang X (2014) Preparation of magnetic ionic liquid/chitosan/graphene oxide composite and application for water treatment. *Int J Biol Macromol* 66:172–178. <https://doi.org/10.1016/j.ijbiomac.2014.02.031>
- Liu M, Chen C, Wen T, Wang X (2014) Synthesis of magnetic ion-imprinted composites and selective separation and preconcentration of U(VI). *Dalt Trans* 43:7050–7056. <https://doi.org/10.1039/C3DT53527D>
- Liu M, Tao Z, Wang H, Zhao F, Sun Q (2016) Study on the adsorption of Hg(II) by one-pot synthesis of amino-functionalized graphene oxide decorated with a Fe₃O₄ microsphere nanocomposite. *RSC Adv* 6:84573–84586. <https://doi.org/10.1039/C6RA16904J>
- Madadrang CJ, Kim HY, Gao G, Wang N, Zhu J, Feng H, Goring M, Kasner ML, Hou S (2012) Adsorption behavior of EDTA-graphene oxide for Pb (II) removal. *ACS Appl Mater Interfaces* 4:1186–1193. <https://doi.org/10.1021/am201645g>
- Marcano DC, Kosynkin DV, Berlin JM, Sinitskii A, Sun Z, Slesarev A, Alemany LB, Lu W, Tour JM (2010) Improved synthesis of graphene oxide. *ACS Nano* 4:4806–4814. <https://doi.org/10.1021/nn1006368>
- Mejias Carpio IE, Mangadlao JD, Nguyen HN, Advincula RC, Rodrigues DF (2014) Graphene oxide functionalized with ethylenediamine triacetic acid for heavy metal adsorption and anti-microbial applications. *Carbon* 77:289–301. <https://doi.org/10.1016/j.carbon.2014.05.032>
- Mohammed Abdul KS, Jayasinghe SS, Chandana EPS, Jayasumana C, De Silva PMCS (2015) Arsenic and human health effects: a review. *Environ Toxicol Pharmacol* 40:828–846. <https://doi.org/10.1016/j.etap.2015.09.016>
- Mohan D, Pittman CU (2007) Arsenic removal from water/wastewater using adsorbents—a critical review. *J Hazard Mater* 142:1–53. <https://doi.org/10.1016/j.jhazmat.2007.01.006>
- Moussavi G, Barikbin B (2010) Biosorption of chromium(VI) from industrial wastewater onto pistachio hull waste biomass. *Chem Eng J* 162:893–900. <https://doi.org/10.1016/j.cej.2010.06.032>
- Ohno M, Hayashi H, Suzuki K, Kose T, Asada T, Kawata K (2011) Preparation and evaluation of magnetic carbonaceous materials for pesticide and metal removal. *J Colloid Interface Sci* 359:407–412. <https://doi.org/10.1016/j.jcis.2011.04.036>
- Okeyo A, Nontongana N, Fadare T, Okoh A (2018) Vibrio species in wastewater final effluents and receiving watershed in south africa: implications for public health. *Int J Environ Res Public Health* 15:1266. <https://doi.org/10.3390/ijerph15061266>
- Orisakwe OE, Asomugha R, Afonne OJ, Anisi CN, Obi E, Dioka CE (2004) Impact of effluents from a car battery manufacturing plant in nigeria on water, soil, and food qualities. *Arch Environ Heal* 59:31–36. <https://doi.org/10.3200/AEOH.59.1.31-36>
- Pandey PK, Choubey S, Verma Y, Pandey M, Chandrashekhar K (2009) Biosorptive removal of arsenic from drinking water. *Bioresour Technol* 100:634–637. <https://doi.org/10.1016/j.biortech.2008.07.063>
- Raghu MS, Yogesh Kumar K, Prashanth MK, Prasanna BP, Vinuth R, Pradeep Kumar CB (2017) Adsorption and antimicrobial studies of chemically bonded magnetic graphene oxide-Fe₃O₄ nanocomposite for water purification. *J Water Process Eng* 17:22–31. <https://doi.org/10.1016/j.jwpe.2017.03.001>
- Ranjan Rout D, Mohan Jena H (2021) Synthesis of novel reduced graphene oxide decorated β -cyclodextrin epichlorohydrin composite and its application for Cr(VI) removal: Batch and fixed-bed studies. *Sep Purif Technol* 278:119630. <https://doi.org/10.1016/j.seppur.2021.119630>
- Saha B, Baek S, Lee J (2017) Highly sensitive bendable and foldable paper sensors based on reduced graphene oxide. *ACS Appl Mater Interfaces* 9:4658–4666. <https://doi.org/10.1021/acsami.6b10484>
- Saha B, Purwar P, Lee J, Saha S (2018) Magnetic nanoparticle encapsulation for the manipulation of bacterial movement and spontaneous detection by reduced graphene oxide. *Adv Biosyst* 2:1800095. <https://doi.org/10.1002/adbi.201800095>
- Shahzad A, Miran W, Rasool K, Nawaz M, Jang J, Lim S-R, Lee DS (2017) Heavy metals removal by EDTA-functionalized chitosan graphene oxide nanocomposites. *RSC Adv* 7:9764–9771. <https://doi.org/10.1039/C6RA28406J>
- Sharif HMA, Mahmood A, Cheng H-Y, Djellabi R, Ali J, Jiang W-L, Wang S-S, Haider MR, Mahmood N, Wang A-J (2019) Fe₃O₄ nanoparticles coated with EDTA and Ag nanoparticles for the catalytic reduction of organic dyes from wastewater. *ACS Appl Nano Mater* 2:5310–5319. <https://doi.org/10.1021/acsanm.9b01250>
- Shen YF, Tang J, Nie ZH, Wang YD, Ren Y, Zuo L (2009) Preparation and application of magnetic Fe₃O₄ nanoparticles for wastewater purification. *Sep Purif Technol* 68:312–319. <https://doi.org/10.1016/j.seppur.2009.05.020>
- Singh TS, Pant K (2004) Equilibrium, kinetics and thermodynamic studies for adsorption of As(III) on activated alumina. *Sep Purif Technol* 36:139–147. [https://doi.org/10.1016/S1383-5866\(03\)00209-0](https://doi.org/10.1016/S1383-5866(03)00209-0)
- Sun L, Yu H, Fugetsu B (2012) Graphene oxide adsorption enhanced by in situ reduction with sodium hydrosulfite to remove acridine orange from aqueous solution. *J Hazard Mater* 203–204:101–110. <https://doi.org/10.1016/j.jhazmat.2011.11.097>
- Terdputtakun A, Arqueropanyo O, Sooksamiti P, Janhom S, Naksata W (2017) Adsorption isotherm models and error analysis for single and binary adsorption of Cd(II) and Zn(II) using leonardite as adsorbent. *Environ Earth Sci* 76:777. <https://doi.org/10.1007/s12665-017-7110-y>
- Verma RP, Sahu PS, Rathod M, Mohapatra SS, Lee J, Saha B (2022) Ultra-sensitive and highly stretchable strain sensors for monitoring of human physiology. *Macromol Mater Eng* 307:2100666. <https://doi.org/10.1002/mame.202100666>
- Vieira RS, Beppu MM (2006) Dynamic and static adsorption and desorption of Hg(II) ions on chitosan membranes and spheres. *Water Res* 40:1726–1734. <https://doi.org/10.1016/j.watres.2006.02.027>
- Wang J, Guo X (2020) Adsorption isotherm models: classification, physical meaning, application and solving method. *Chemosphere* 258:127279. <https://doi.org/10.1016/j.chemosphere.2020.127279>
- Weerasundara L, Ok Y-S, Bundschuh J (2021) Selective removal of arsenic in water: a critical review. *Environ Pollut* 268:115668. <https://doi.org/10.1016/j.envpol.2020.115668>
- Zhao D, Zhang Q, Xuan H, Chen Y, Zhang K, Feng S, Alsaedi A, Hayat T, Chen C (2017) EDTA functionalized Fe₃O₄/graphene oxide for efficient removal of U(VI) from aqueous solutions. *J Colloid Interface Sci* 506:300–307. <https://doi.org/10.1016/j.jcis.2017.07.057>
- Zhao G, Li J, Ren X, Chen C, Wang X (2011) Few-layered graphene oxide nanosheets as superior sorbents for heavy metal ion

- pollution management. *Environ Sci Technol* 45:10454–10462. <https://doi.org/10.1021/es203439v>
- Zhou L, Ji L, Ma P-C, Shao Y, Zhang H, Gao W, Li Y (2014) Development of carbon nanotubes/CoFe₂O₄ magnetic hybrid material for removal of tetrabromobisphenol A and Pb(II). *J Hazard Mater* 265:104–114. <https://doi.org/10.1016/j.jhazmat.2013.11.058>
- Zhou L, Jin J, Liu Z, Liang X, Shang C (2011) Adsorption of acid dyes from aqueous solutions by the ethylenediamine-modified magnetic chitosan nanoparticles. *J Hazard Mater* 185:1045–1052. <https://doi.org/10.1016/j.jhazmat.2010.10.012>
- Zhou M, Wei Z, Qiao H, Zhu L, Yang H, Xia T (2009) Particle size and pore structure characterization of silver nanoparticles prepared by confined arc plasma. *J Nanomater* 2009:1–5. <https://doi.org/10.1155/2009/968058>

Publisher's note Springer Nature remains neutral with regard to jurisdictional claims in published maps and institutional affiliations.